

TOPOGRAPHIC CORRECTION OF THE REMOTE SENSING DATA

M. Sc. Beata HEJMANOWSKA
University of Mining and Metallurgy in Cracow, POLAND
now: Technische Universität Clausthal, GERMANY

ISPRS Commission II

ABSTRACT

Reduction of the topographic effect from remote sensing data might be necessary before the following image processing (classification, mathematic modelling etc.). Radiance that depends upon target photometric characteristic and geometry of illumination and registration can be described by bidirectional radiation distribution function (BRDF). The photometric function of the objects is made up by micro- and macrostructure of their surface. It determines the type of scattering that can be forward, isotropic or back. In this paper the short literature review is made (1930 - 1991). The program written by author was used to compare the three type of scattering for different slope, exposure and season. Example of the topographic correction of Landsat data is presented.

INTRODUCTION

Level of the registered electromagnetic radiation very often depends on the terrain topography. Reduction of the topography effect from satellite, airborne and ground remote sensing data is very important for albedo or temperature calculation. In many cases, different albedo or different temperature calculated from remote sensing data are caused only by topographic effect. Radiation, reflected from the surface, depends on the macrostructure of the surfaces and on the microscattering properties of the individual surface elements. A macrostructure can be classified as smooth, corrugated or porous. The microscattering properties can be divided into three general types: forward-scatter, isotropic or backscatter. Some authors have concentrated on the experimental determination of surface reflectance properties (Hapke et al 1963a, Coulson 1966, Watson 1972, Suits 1977, Kriebel 1977, Koepke et al 1978, Kimes et al 1980, Richardson 1981). Besides, many theoretical models of BRDF (Bidirectional Reflectance Distribution Function) have been developed (Hapke 1963b, Torrance et al 1967, Emslie et al 1972).

BACKGROUND

The mechanism of reflection is fully described by the BRDF. The BRDF denoted by symbol f_r is defined as the ratio of reflected radiance, dL_r , in the direction of sensor to the irradiance, dE_o , in the direction toward the source, i.e.:

$$f_r = \frac{dL_r(V_o, A_o, V_r, A_r)}{dE_o(V_o, A_o)} \quad (1)$$

where:

V_o, A_o - zenith illumination angle and azimuth,
 V_r, A_r - zenith angle and azimuth of the direction of the sensor.
The radiance of the target with a given BRDF can thus be computed according to:

$$L_r = \int_{\text{hemisphere}} f_r dE_o \quad (2)$$

Estimation of factor f_r is necessary for topographic correction of the remote sensing data. Many experiments have been performed to describe BRDF of different objects.

On the base on the literature review can be concluded that:

1. Individual surface elements can scatter electromagnetic radiation incoming to the surface: **forward, isotropic and back.**

Particles of size comparable with or less than wavelength of light **forward scatter** because of diffraction. Transparent particles forward-scatter also because refraction and focusing effects and back-scatter by internal reflection. The ray reflected from such surfaces, with forward (specular) microstructure properties, lie in plane formed by the incident ray and the surface normal and make an angle with local normal equal to the angle between the incident ray and the local normal. **Isotropic scattering** is attributed to translucent objects which have many irregularities and inhomogenities on their surface or in their interior. The ray of light can penetrate into such objects in any direction. Small particles of rocks and other dielectrics usually scatter the light in this way. Opaque objects with smooth surface orientated randomly also have an average microscattering law that is isotropic; examples are polished metal spheres and randomly orientated dark crystals whose surface are smooth clearance plans. Objects with isotropic macrostructure reflect light equal in all directions. A **broad back scatter** type of microscattering law is exhibited by opaque objects with somewhat rough surface, such as a piece of rocks several millimeters or more in size, for such an object appears brightest to an observer when the source of light is directly behind him so that he sees only the illuminated face, and is less bright if he views it at any other angle so that he also sees shadowed areas.

2. **Surfaces of high albedo** reflect light diffusively and it is independent of microscattering properties and macrostructure of the surface because the ray are usually multiply reflected.

3. **Surface of low albedo**, when albedo decrease below about 25%, can reflect light in different way. It depends on microscattering properties and macrostructure of the surface. Dark surfaces with smooth macrostructure reflect light in to a broad specular peak. The reflection from dark corrugated surfaces depends on microscattering properties. It means that such surfaces can reflect light in pseudospecular, isotropic and back manner, when it is built with forward, isotropic or back scattering elements. Dark porous surfaces with forward scattering microstructure have broad pseudospecular peak and a backscattering peak. If the objects are isotropic scatters the surface reflects light in broad backscatter peak, whereas if the microscattering properties are of the backscatter class the surface backscatter light sharply. At the same times, many theoretical models have been developed to describe reflection from different surfaces. The most popular is the Torrance-Sparrow's specular model and Hapke's backscattering model. Besides, three others models, base on Lambert, Lommel-Seelinger and Euler formulas are known (Petit et al 1930).

Fig.1 and Fig.2 present BRDF calculated on the base of mentioned above models for two illumination angles. Furthermore the simplest specular model, proposed by author, is on these figure shown.

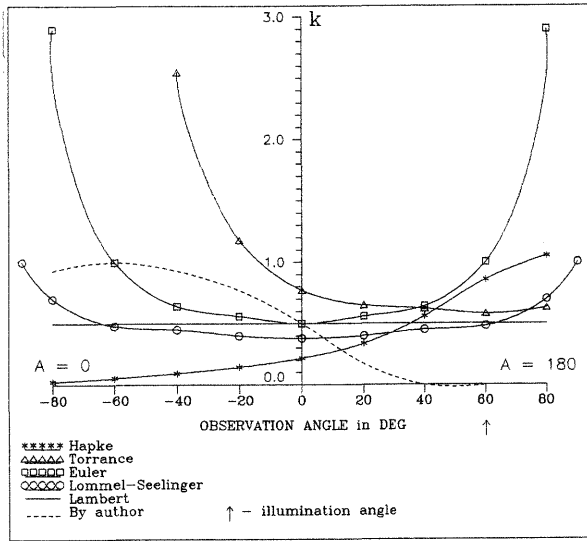


Fig.1 BRDF in plane of incident ray (illumination angle 60°)

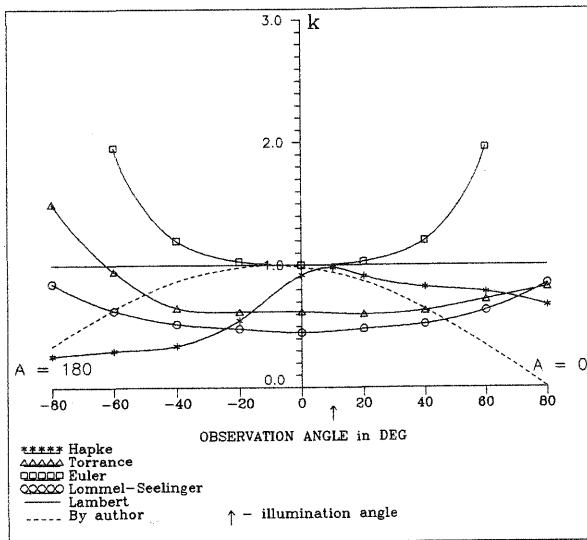


Fig.2 BRDF in plane of incident ray (illumination angle 10°)

TOPOGRAPHIC CORRECTION OF REFLECTED RADIATION

The correction method presented below bases on the assumption that the wanted radiation level is the radiation reflected from horizontal surfaces. It means that after transformatin we should obtain the radiation level as it would be when the terrain is horizontal. To remove negative topographic effect we need to know the solar illumination conditions of sloping surfaces. First, we need the slope and exposure of sloping surfaces. On a digital terrain grid slope (S) and azimuth (A) of the surfaces can be founded numerically :

$$\tan S = \left(\frac{\delta Z}{\delta x} \right)^2 + \left(\frac{\delta Z}{\delta y} \right)^2 \quad (3)$$

$$\tan A = - \left(\frac{\delta Z}{\delta y} \right) / \left(\frac{\delta Z}{\delta x} \right) \quad (4)$$

The equation for calculation of illumination angles on sloping surface are following:

$$\cos V_o = \cos V_s \cdot \cos S + \sin V_s \sin S \cos (A_s - A) \quad (5)$$

$$\tan A_o = \frac{\sin V_s \sin (A_s - A)}{[\sin V_s \cos S \cos (A_s - A) - \cos V_s \sin S]} \quad (6)$$

where:

V_o, A_o - illumination angle and azimuth on sloping surface,
 S, A - slope and exposure of the surface,
 V_s, A_s - solar zenith angle and azimuth on horizontal surface.
 Using program TOPOGRAPH, written by author, the following correction factors was compared for different slope, exposure and season:

$$k^L = \frac{\cos V_s}{\cos V_o} \quad (\text{diffusively scattering - Lambert's model})$$

$$k^H = \frac{\cos V_s (\cos V_o + \cos S)}{\cos V_o (1 + \cos V_s)} \quad (\text{backscattering - Hapke's model})$$

$$k^S = \frac{\cos \beta \cos S}{\cos (V_o \pm \beta)} \quad (\text{specular model})$$

where: β - angle between edge of intersection of surface normal and incident flat and horizontal flat, $\beta = f(S, A, V_s, A_s)$. To compare, the other correction factor, developed by Minnaert, was tested:

$$k^M = \frac{\cos^K V_s}{\cos^K V_o \cos^{K-1} S}$$

where : K - parameter which depends on surface roughnes; when K=1 the Minnaert's model becomes Lambertian model, when K is less 1 it becomes more or less the backscattering model.

Result of the test calculation

All test calculation was performed for latitude 50N. Table 1 contains the boundary illumination conditions for surfaces with different exposure in different season (boundary slopes above which N, NW, NE exposure are not illuminated; S, SW, SE facing slopes are illuminated always).

Table 1 Boundary illumination conditions for northerly - facing slopes (latitude 50° N, local noon).

Month	V_s	S_N	S_{NE}	S_{NW}
02	61°	20°	30°	30°
03	52°	30°	40°	40°
04	40°	40°	50°	50°
05	33°	50°	60°	60°
06	27°	60°	60°	60°
07	29°	60°	60°	60°
08	36°	50°	60°	60°
09	48°	40°	50°	50°
10	58°	30°	30°	40°
11	68°	20°	20°	30°
12	73°	10°	20°	20°

Boundary illumination angles and correction factors for northerly-facing surfaces are presented in Table 2, for southerly-facing surfaces in Table 3.

Tab.2 Boundary illumination angles and correction factors for northerly- facing surfaces.

Month	S (N)	$k^l(N)$	$k^l(NW NE)$	$k^h(N)$	$k^h(NW NE)$	$k^m(N)$	$k^m(NW NE)$	$S^s(N)$	$k^s(N)$	$k^s(NW NE)$
02	10°	1.5	1.3	1.31	1.20	1.069	1.045	10°	3.1	2.0
03	20°	1.9	1.6	1.54	1.31	1.092	1.045	10°	2.0	1.5
04	30°	2.2	1.7	1.53	1.29	1.047	0.997	20°	4.4	2.6
05	40°	2.9	2.0	1.65	1.33	0.998	0.938	20°	2.9	2.1
06	50°	4.0	2.7	1.81	1.40	0.925	0.859	20°	2.3	1.8
07	50°	4.6	2.9	2.04	1.45	0.952	0.870	20°	2.4	1.4
08	40°	3.3	2.4	1.86	1.50	1.029	0.956	20°	3.3	2.3
09	30°	3.2	2.1	2.01	1.22	1.128	1.035	10°	1.8	1.5
10	20°	2.5	1.8	1.91	1.40	1.147	1.070	10°	2.5	1.8
11	10°	1.8	1.4	1.56	1.35	1.110	1.070	-	-	-

S(N) - slope of surface with N exposure for which the correction factor is maximum in Lambert's, Hapke's and Minnaert's models,

$S^s(N)$ - slope of surface with exposure for which the correction factor is maximum in specular model,

$k^{(h,m,s)}(N)$ - maximum of correction factor in Lambert's (Hapke's, Minnaert's and specular models) for N exposures,

$k^{(h,m,s)}(NW NE)$ - maximum of correction factor in Lambert's (Hapke's, Minnaert's and specular models) for NW and NE exposures.

Tab.3 Boundary illumination angles and correction factors for southerly-facing surfaces.

Month	S^l	k^l	S^h	k^h	S^m	k^m	S^s	k^s
02	60°	0.49	80°	0.39	80°	0.216	30°	0.493
03	50°	0.62	80°	0.46	80°	0.229	30°	0.621
04	40°	0.77	80°	0.53	80°	0.246	20°	0.766
05	30°	0.84	80°	0.57	80°	0.257	20°	0.845
06	30°	0.89	80°	0.61	80°	0.267	10°	0.898
07	30°	0.88	80°	0.60	80°	0.263	10°	0.885
08	40°	0.81	80°	0.56	80°	0.252	20°	0.811
09	50°	0.68	80°	0.49	80°	0.236	20°	0.682
10	60°	0.53	80°	0.41	80°	0.220	30°	0.529
11	70°	0.37	80°	0.32	80°	0.203	30°	0.377
12	70°	0.29	80°	0.27	80°	0.193	40°	0.294

$S^{(h,m,s)}$ - slope of southerly-facing surfaces for which the correction factor is minimum in Lambert's (Hapke's, Minnaert's and specular) model,

$k^{(h,m,s)}$ - minimum of the correction factor for southerly-facing surfaces in Lambert's (Hapke's, Minnaert's and specular) model.

Fig.3 ÷ 6 show relation between albedo correction factor, slope and season for different exposure in Lambert's, Hapke's, Minnaert's ($k=0.2$) and specular models.

As summary of the test calculation can be stated :

1. **Northerly-facing surfaces** can be darker or brighter than horizontal surfaces that depends on the type of scattering. In Lambert's model correction factor increase with slope from 1.0 to 4.6. In summer $k^l(N)_{max} = 3.7$ and $k^l(WE NE)_{max} = 2.5$. In Hapke's model correction factor increase with slope from 1.0 to 2.0. In summer and autumn $k^h(N)_{max} = 2.0$ and $k^h(NW NE)_{max} = 1.45$. In spring $k^h(N)_{max} = 1.5$ and $k^h(NW NE)_{max} = 1.3$. Slope for maximum value of correction factor for Lambert's and Hapke's models is equal about 45° in summer. According to Minnaert's model the such surfaces can be darker or brighter than horizontal surfaces, $k^m(N NW NE) = (0.8 - 1.1)$. In spring and autumn $k^m(N)$ increase with slope but $k^m(NW NE)$ decrease with slope. In summer reversely, $k^m(N)$ decrease with slope and $k^m(NW NE)$

increase with slope. In specular model correction factor $k^s(N NW NE)$ increase with slope from 1.0 to 4.4. In summer $k^s(N)_{max}$ appears for slope 20° and is equal 2.5 ($k^s(NW NE)_{max} = 2.0$).

2. **Southerly-facing surfaces** corrected using Lambert's model can be brighter or darker than horizontal surfaces. Factor k^l for such surfaces can change from 0.3 to 1.9. In spring and autumn $k^l < 1$ for all S, SW, SE exposures and slopes. In summer $k^l < 1$ when slope is less than about 40°. k^s appears for slope 70° in December (0.29) and for slope 30° in summer (0.89). In Hapke's model, southerly-facing surfaces are always brighter than horizontal, k^h decrease with slope from (1.0 to 0.27). Maximum of k^h appears always for slope 80°. Difference between k^h for slope 10° and slope 80° is independent of season and equal about 0.4 ($k^h(10°) = 2 k^h(80°)$). The correction using Minnaert's model of such surfaces is similar to Hapke's correction. k^m decrease with slope from 1.0 to 0.3 and k^m appears for slope 80°. Correction factor in specular model can be from range (0.3-3.7). In summer $k^s < 1$,

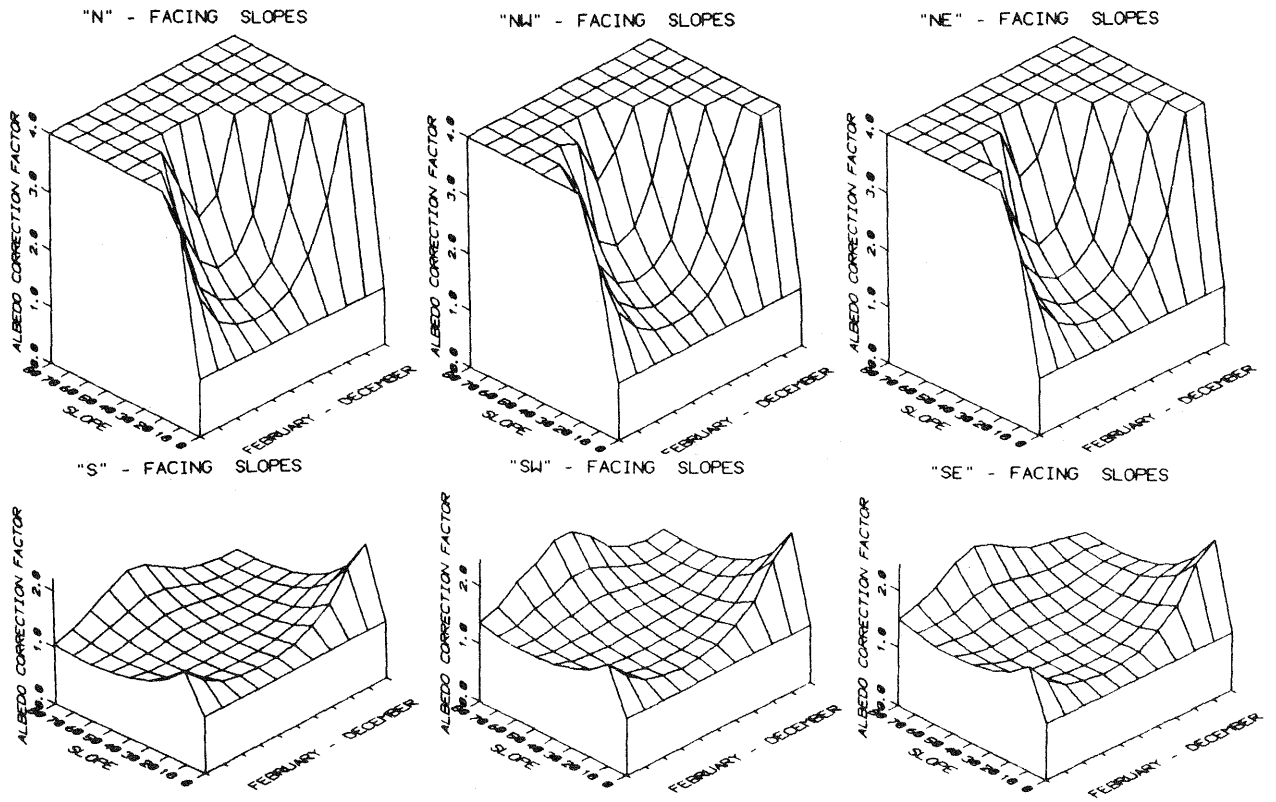


Fig.3 Relation between albedo correction factor, slope and season for different exposure (Lambert's model).

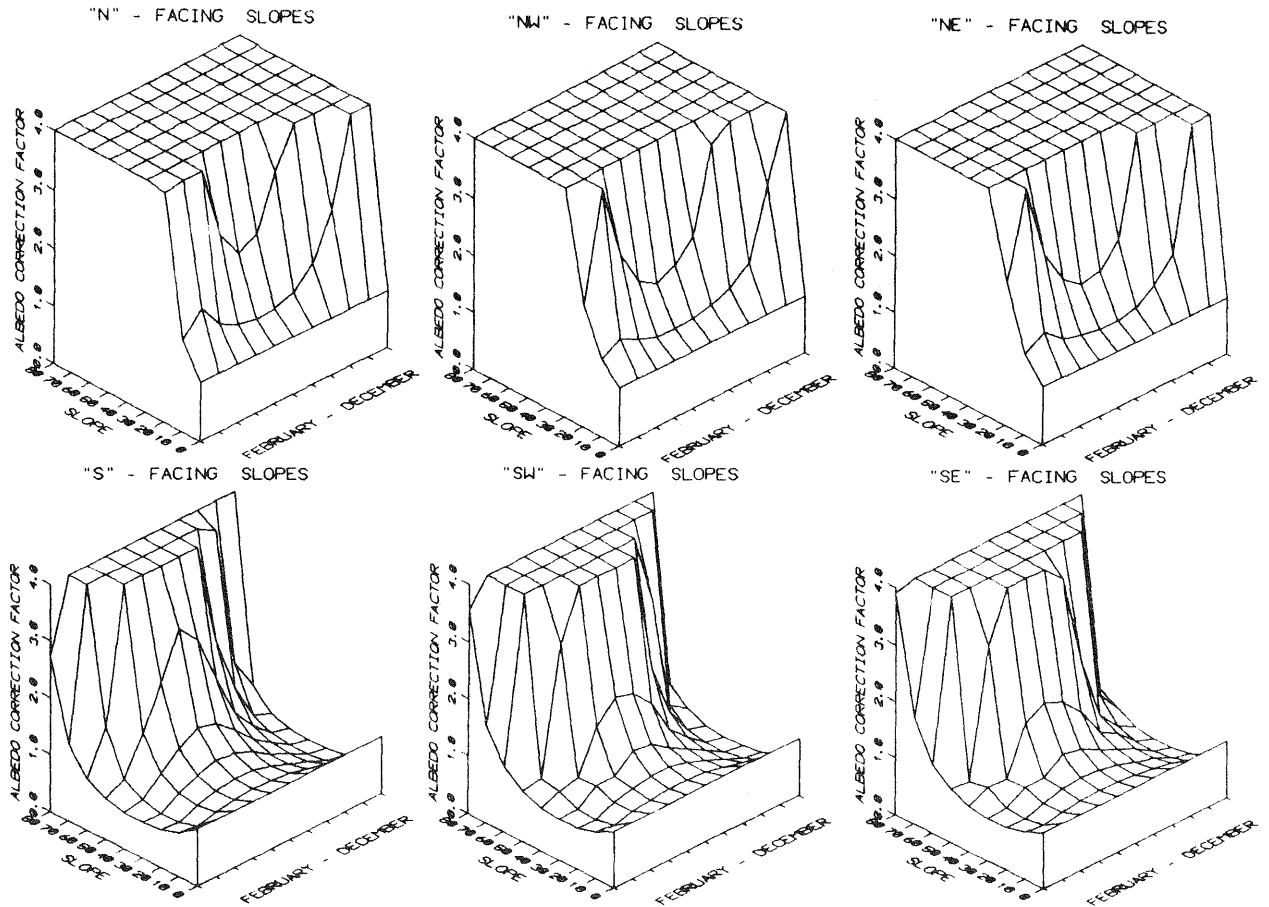


Fig.4 Relation between albedo correction factor, slope and season for different exposure (specular model)

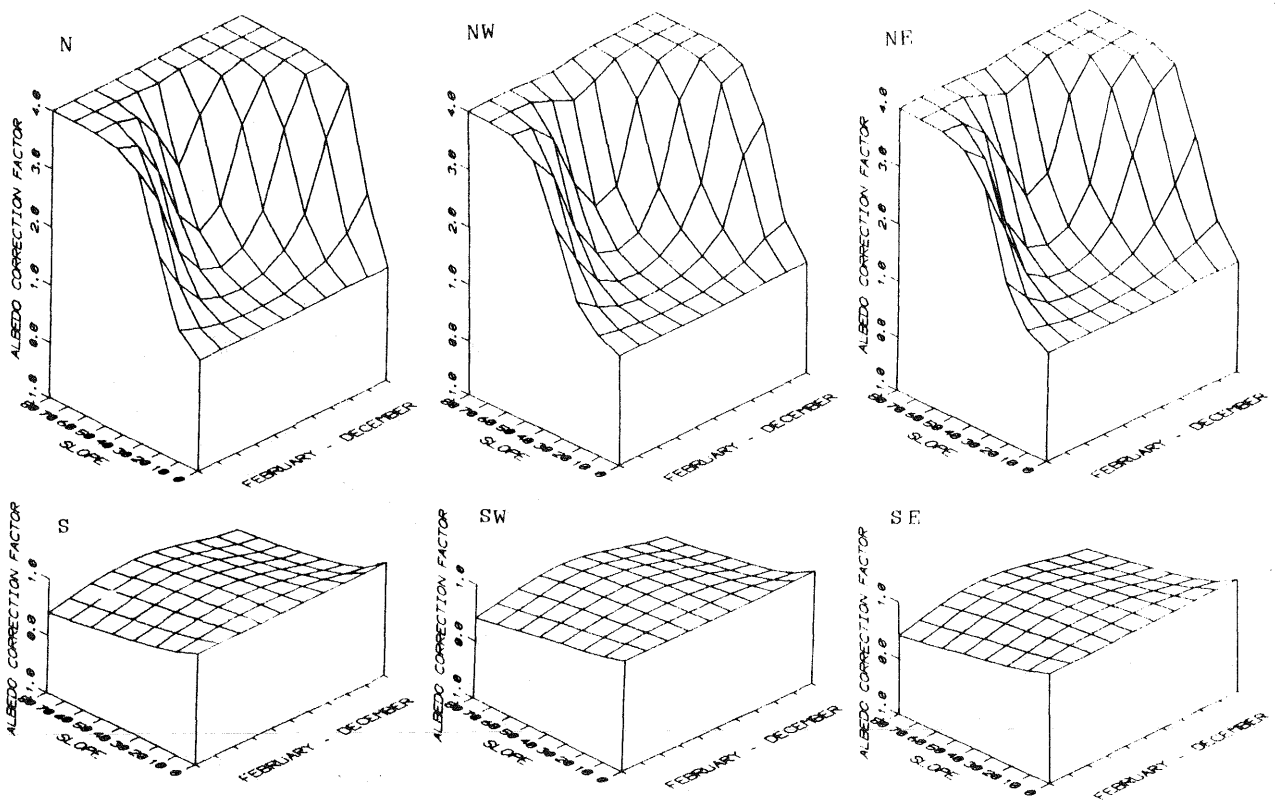


Fig.5 Relation between albedo correction factor,slope and season for different exposure (Hapke's model)

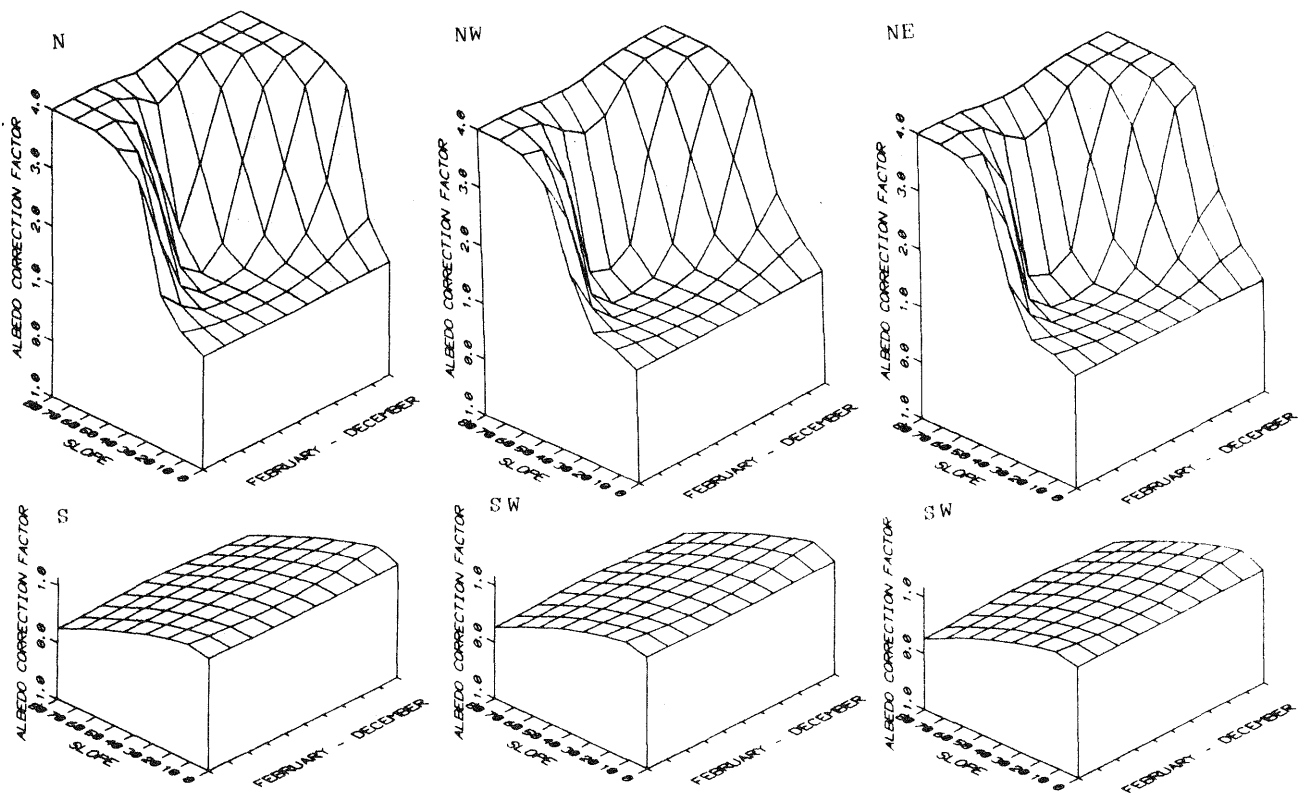


Fig. 6 Relation between albedo correction factor, slope and season for different exposure (Minnaert's model, $k=0.2$)

when slope is less 30° .

3. Eastern and western exposure in Lambert's model are always darker than horizontal surfaces. k^t (E W) increase with slope from 1.0 to 3.0. In Hapke's model correction factor for such surfaces fluctuate near 1.0. According to Minnaert's model correction factor decrease with slope from 1.0 to 0.3. Correction factor in specular model increase with slope from 1.0 to 2.5.

TOPOGRAPHIC CORRECTION OF THERMAL RADIATION

The topographic correction of thermal radiation that have been performed based on the same assumption like formerly that the desirable thermal radiation level is the radiation of horizontal surfaces. The following thermal correction coefficient was tested:

$$k^t = \frac{\cos(V_g)}{\cos(V_o) \cos(S)} \quad (12)$$

Fig.7 shows relation between thermal correction coefficient, slope and season for different exposure.

In table 4 boundary illumination angles and thermal correction factors for surface with northern and southern exposures are presented (symbols like in table 2, 3).

Table 4. Boundary illumination angles and thermal correction factors for surface with northern an southern exposures.

month	S(N)	k(N)	k ^t (NW NE)	S(S)	k(S)
02	10°	1.5	1.4	30°	0.650
03	20°	2.1	1.7	20°	0.772
04	30°	2.6	2.0	20°	0.868
05	40°	3.7	2.7	20°	0.916
06	50°	6.2	4.2	10°	0.946
07	50°	7.1	4.5	10°	0.939
08	40°	4.4	3.0	20°	0.896
09	30°	3.8	2.5	20°	0.814
10	20°	2.7	2.0	30°	0.691
11	10°	1.8	1.5	30°	0.547
12	-	-	-	40°	0.455

As a summary can be stated the following conclusion:

1. Northerly-facing slopes are colder than horizontal, k^t (N) = (1.0 - 7.1). In June and July maximum value of k^t is equal about 6.5 for slopes 50° , in May, August and September about 4.0 for slope 30° , in March April and October about 2.5 for slope 25° . For exposere NW and NE k^t is about 60 % in summer and 75 % - 80 % in spring and outum less than for N exposeres.
2. Southerly-facing slopes can be warmer or colder than horizontal surfaces, k^t (S) = (0.5 - 11.0). k^t increase with slope. In summer slope above which factor $k^t > 1$ is about 30° .
3. Factor k^t for W,E exposures increase with slope, k^t (E W) = (1.0 - 12.0) .

TOPOGRAPHIC CORRECTION OF LANDSAT TM DATA

A study area (5km x 6km) is situated west of Frankfurt am Main (Germany), near Hochheim am Main (Fig. 8). Landsat TM data, recorded on 30 July 1984, were supplied by IFAG (Institut für Angewandte Geodäsie) in Frankfurt. The data were preprocessed with the support of Institut für Planungsdaten Offenbach, Hessisches Landesvermessungsamt Wiesbaden and Institut für Photogrammetrie und Ingenieurvermessungen, der Universität Hannover by IFAG . For Landsat multispectral data this com-

prise the following operation: rectification (ground control points, polynominals), resampling (indirect, nearest neighbourhood, 25 m), and size file formation (1024 records with 1120 pixels each). Next, with support of Institut of Meteorology and Water Menegement, Cracow (Poland) the Computer Compatible Tape (CCT, 1600 BPI) were recopied on 5.25" floppy diskettes 1.2 MB and BSQ format was preserved. Topographic map was digitized (by hand) to obtain numerical terrain model (Fig.9). Using the program TOPOGRAPH the specular albedo correction coefficient (Fig.10) and thermal correction coefficient (Fig.11) were for the study area simulated. Landsat TM, channel 6 (thermal), before and after correction are shown on Fig.12,13. Fig.14,15 show differences between images before and after correction (TM 6 and TM 3).

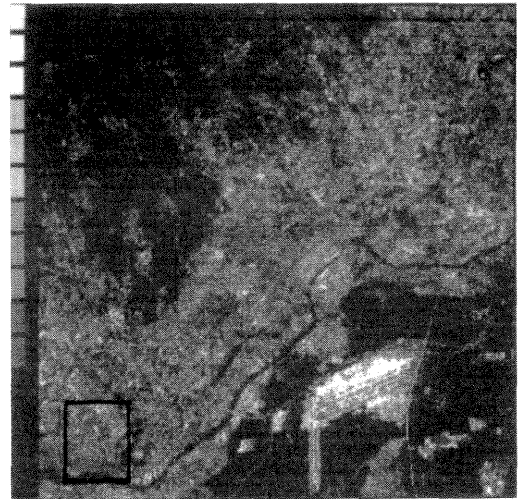


Fig. 8 Test area.

SURFACE TOPOGRAPHY (Hochhe (m) a/Me (in))

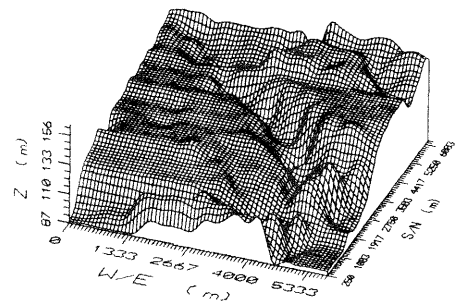


Fig. 9 Surface topography.

ALBEDO CORRECTION COEFFICIENT

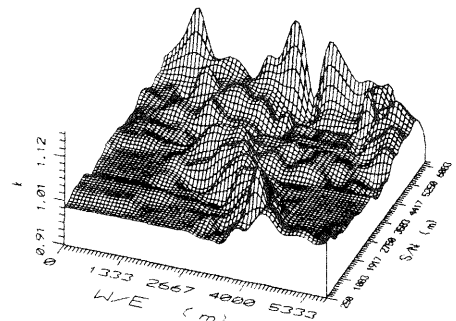


Fig. 10 Albedo correction factor (specular model).

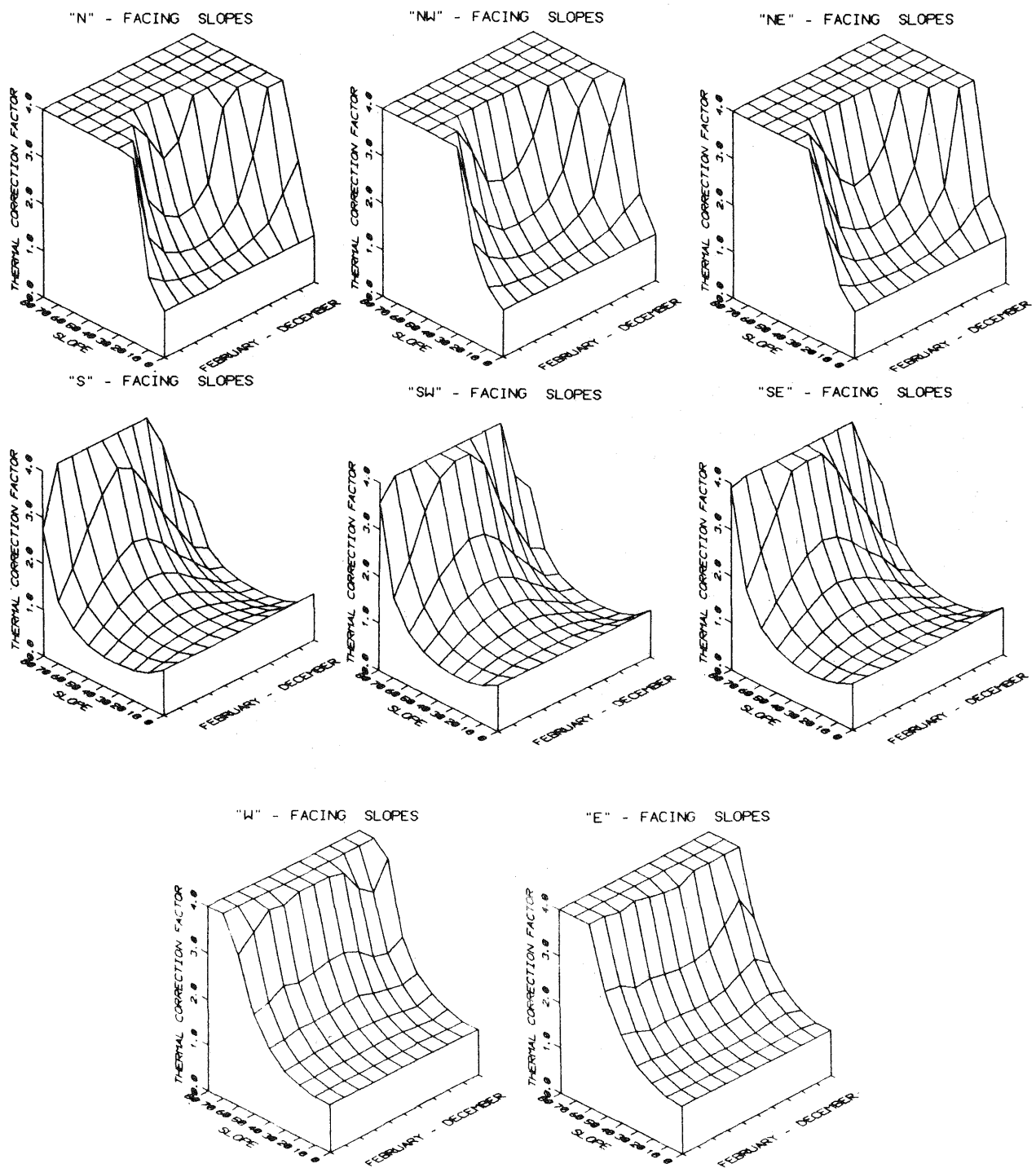


Fig. 7 Relation between thermal correction factor, slope and season for different exposure.

THERMAL CORRECTION COEFFICIENT

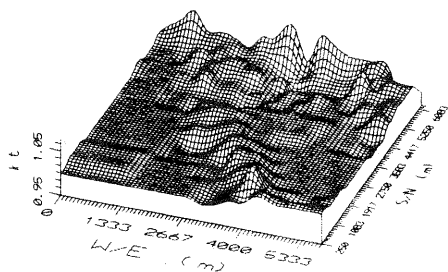


Fig.11 Thermal correction factor.

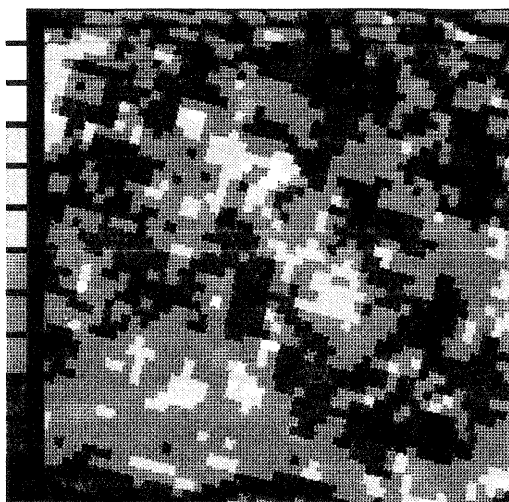


Fig.12. TM6 before correction.

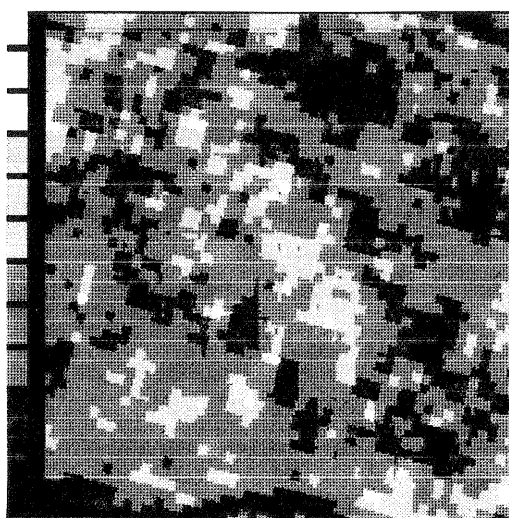


Fig. 13 TM 6 after correction.

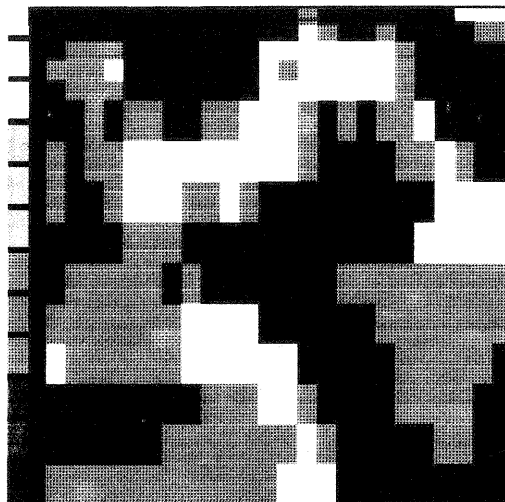


Fig.14 Difference between TM6 before and after correction, (white, grey, black - area before correction warmer, the same, colder than after correction)

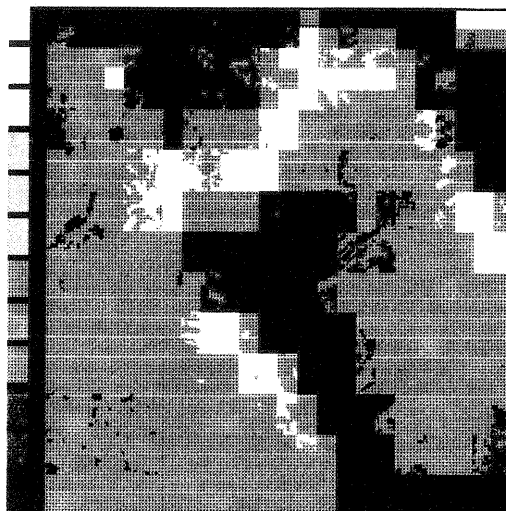


Fig.15. Difference between TM3 before and after correction (white, grey, black - area before correction brighter, the same, darker than after correction).

CONCLUSIONS

Before image processing or mathematic modelling might be necessary to remove the topographic effect from the raw data. The correction should be performed separately for different covers of the surface. Surface can reflect light: forward, isotropic and back that depends on micro- and macrostructure. The program TOPOGRAPH written by author was used to test of these type of scattering for different slope, exposure of the surface and season. The correction factor was calculated on the base of assumption that we want to transform the raw image (f.ex. some of Landsat TM channels) to the image as it would be when terrain is horizontal. Correction coefficient for different slopes and season was calculated on the base of Lambert's, Hapke's, Minnaert's ($k=0.2$) and specular scattering models. All calculation was made for latitude 50N. Results are presented graphically. It should be mentioned that the correction is possible when the surface is illuminated, so the boundary illumination conditions and respectively boundary correction factors can be founded. In Lambert's model correction factor can change in range (0.3-4.6), in Hapke's model in range (0.27-2.0), in Minnaert's model in range (0.3-1.1), in specular model in range (0.3-4.4). Northerly -

facing slopes can be only darker than horizontal surface in Lambert's, Hapke's and specular models. According to Minnaert's model such surfaces can be darker or brighter than horizontal. Southerly - facing slopes in Lambert's and specular models can be darker or brighter than horizontal, that depends on slope. In Hapke's and Minnaert's models such surface are always brighter than horizontal surfaces. Slope with eastern and western exposure are in Lambert's and specular model darker than horizontal surface, in Minnaert's reversely.

In this paper the thermal correction coefficient was also proposed and tested. According to formula (12) surface with northern, western and eastern exposure are always colder than horizontal. Correction coefficient can be maximum 12.0. Southerly facing surfaces can be warmer or colder than horizontal, that depends on slope.

Besides, the example of the topographic correction of Landsat TM was presented. The difference in height of the surface was only 30 m, the slopes were not significant therefore albedo, and thermal correction coefficient were small (0.92-1.12, 0.95-1.05). To obtain the digital terrain the model topographic map was digitized by hand, so the resolution was not sufficiently to suitable topographic correction. However the results of albedo and thermal correction can be easy seen of the figures.

REFERENCES

- Civco, D.L., 1989. Topographic Normalization of Landsat Thematic Mapper Digital Imagery. *Photogrammetry Engineering and Remote Sensing*, 55 (9): 1303-1309.
- Colby, J.D., 1991. Topographic Normalization in Rugged Terrain. *Photogrammetry Engineering and Remote Sensing*, 57 (5): 531-537.
- Coulson, K.L., 1966. Effects of Reflection Properties of Natural Surfaces in Aerial Reconnaissance. *Applied Optics*, 5 (6): 905-917
- Dozier, J., Frew, J., 1990. Rapid Calculation of Terrain Parameters For Radiation Modelling From Digital Elevation Data. *IEEE Transactions on Geoscience and Remote Sensing*, 28 (5): 963-969.
- Egbert, D.D., Ulaby, F.T., 1972. Effects of Angles on Reflectivity. *Photogrammetry Engineering and Remote Sensing*.....: 556-565
- Emslie, A.G., Aronson, J.R., 1972. Spectral Reflectance and Emittance of Particulate Materials. 1: Theory. *Applied Optics*, 12 (11): 2563-2572.
- Franklin, J., Logan, T.L., Woodcock, L.C.E., Strahler, A.H., 1986. Coniferous Forest Classification and Inventory Using Landsat Digital Terrain Data. *IEEE Transactions on Geoscience and Remote Sensing*, GE-24 (1): 139-149
- Hapke, B., Van Horn, H., 1963a. Photometric Studies of Complex Surfaces, with Application to the Moon. *Journal of Geophysical Research*, 68: 4545-4570.
- Hapke, B.W., 1963b. A Theoretical Photometric Function for the Lunar Surface. *Journal of Geophysical Research*, 68 (15): 4571 -4586
- Holben, B.N., Justice, Ch.O., 1980. The Topographic Effect on Spectral Response from Nadir - Pointing Sensors. *Photogrammetry Engineering and Remote Sensing*, 46 (2): 1191-1200.
- Horn, B.K.P., Sjoberg, R.W., 1979. Calculating the reflectance map. *Applied Optics*, 18 (11): 1770-1779.
- Hugli, H., Frei, W., 1983. Understanding Anisotropic Reflectance in Mountainous Terrain. *Photogrammetry Engineering and Remote Sensing*, 49 (5): 671-683.
- Kimes, D.S., Smith, J.A., Ranson, K.J., 1980. Vegetation Reflectance Measurements as a Function of Solar Zenith Angle. *Photogrammetry Engineering and Remote Sensing*, 46 (12): 1563-1573.
- Kimes, D.S., Kirchner, J.A., 1981. Modelling the Effects of Various Radiant Transfer in Mountainous Terrain on Sensor Response. *IEEE Transactions on Geoscience and Remote Sensing*, GE-19 (2): 100-107.
- Kirchner, J.A., Youkhana, S., Smith, J.A., 1982. Influence of Sky Radiance Distribution on the Ratio Technique for Estimating Bidirectional Reflectance. *Photogrammetry Engineering and Remote Sensing*, 48 (6): 955-959.
- Koebke, P., Kriebel, K.T., 1978. Influence of measured reflection properties of vegetated surfaces on atmospheric radiance and its polarization. *Applied Optics*, 17 (2): 260-264.
- Kowalik, W.S., Lyon, R.J.P., Switzer, P., 1983. The Effects of Additive Radiance Terms on Ratios of Landsat Data. *Photogrammetry Engineering and Remote Sensing*, 49 (5): 659-669
- Kriebel, K.T., 1977. Measured spectral bidirectional reflection properties of four vegetated surfaces. *Applied Optics*, 17 (2): 253-259.
- Leprieur, C.E., Durand, J.M., 1988. Influence of Topography on Forest Reflectance Using Landsat Thematic Mapper and Digital Terrain Data. *Photogrammetry Engineering and Remote Sensing*, 54 (4): 491-496.
- Stohr, Ch.J., West, T.R., 1985. Terrain and Look Angle Effects Upon Multispectral Scanner Response. *Photogrammetry Engineering and Remote Sensing*, 51 (2): 229-235.
- Pettit, E., Nicholson, S.B., 1930. Lunar Radiation and Temperature. *Astrophysical Journal*, 71: 102-193.
- Reeves, R.G., Anson, A., Landen, D., 1975. *Manual of Remote Sensing*. American Society of Photogrammetry, Falls Church, Virginia.
- Richardson, A.J., 1981. Measurement of reflectance factors under daily and intermittent irradiance variations. *Applied Optics*, 20 (19): 3336-3340.
- Ritter, P., 1987. A Vector-Based Slope and Aspect Generation Algorithm. *Photogrammetry Engineering and Remote Sensing*, 53 (8): 1109-1111.
- Smith, J.A., Lin, T.L., Ranson, K.J., 1980. The Lambertian Assumption and Landsat Data. *Photogrammetry Engineering and Remote Sensing*, 46 (9): 1183-1189.
- Smits, G.H., 1972. The Cause of Azimuthal Variations in Directional Reflectance of Vegetative Canopies. *Remote Sensing of Environment*, 2: 175-182.
- Torrance, K.E., Sparrow, E.M., 1967. Theory for off-Specular Reflection From Roughed Surfaces. *Journal of the optical society of America*, 57: 1105-1114.
- Watson, R.D., 1972. Spectral Reflectance and Photometric Properties of Selected Rocks. *Remote Sensing of Environment*, 2: 95-100.